analytical chemistry

Article

Cite This: *Anal. Chem.* 2019, 91, 15644−15651

pubs.acs.org/ac

Toward Development of Fluorescence-Quenching-Based Biosensors for Drought Stress in Plants

Arjun Sharmah,[†] Michael Kraus,[‡,§] Sean R. Cutler,[∥] Justin B. Siegel,[†,§] Siobhan M. Brady,[‡,§] and Ting Guo*[,†]

[†]Department of Chemistry, [‡]Department of Plant Biology and Genome Center, and [§]Genome Center, University of California, Davis, California 95616, United States

[∥]Center for Plant Biology, University of California, Riverside, California 92521, United States

Supporting Information

ABSTRACT: Abscisic acid (ABA) is a drought stress signaling molecule, and simple methods for detecting its levels could benefit agriculture. Here, we present proof-of-concept detection for ABA in aqueous solutions by the use of a mixture of Cyanine 5.5 (Cy5.5) fluorophore- and BHQ3 quencher-conjugated endogenous ABA receptor pyrabactin resistance 1 like proteins (PYL3). These dye-conjugated PYL3 protein form dimers in solutions without ABA and monomerize upon ABA binding. When they are in dimers, fluorescence of Cy5.5 is either nearly completely quenched by the BHQ3 or 20% quenched by another Cy5.5. Consequently, mixtures of equal amounts of the two protein conjugates were used to detect ABA in aqueous solution. As the ABA concentration increased from <1 μM to 1 mM, the intensity of fluorescence detected at around 680 nm from the mixture was more than doubled as a result of ABA-induced monomerization, which leads to halt of quenching and recovery of fluorescence of Cy5.5 in monomers. Kinetic modeling was used to simulate the fluorescence response from the mixture and the results generally agree with the experimentally observed trend. This work demonstrates that fluorescence measurements of a single dissociation reaction in one spectral region are adequate to assess the ABA concentration of a solution.

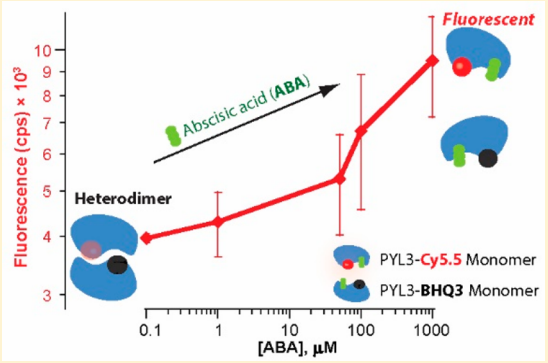

Plants can adjust their growth and development using phytohormones in response to environmental stress. Facing drought or other stressors, for example, plants synthesize and respond to a terpenoid hormone called abscisic acid (ABA), which is involved in seed germination, seedling growth, regulation of stomatal aperture, flowering, and response to pathogens.[1] The ABA signaling network in plants involves a class of water-soluble ABA receptor proteins [PYR (pyrabactin resistance)/PYL (PYR1-like)/RCAR (regulatory components of ABA receptor)], which form dimers in the absence of ABA. Upon ABA binding, the dimers dissociate to their ABA-bound monomeric forms, which then regulate PP2C phosphatases and activate SnRK2 kinases that direct many downstream signaling pathways including the control of stomata aperture.[2,3] In the absence of ABA, the dimeric receptors are autoinhibited, enabling PP2C phosphatases to bind to SnRK2 kinases, rendering them inactive.

Throughout evolution, this response to drought stress has been finely tuned, making it challenging for humans to conveniently detect subtle, yet physiologically relevant changes in ABA concentration without the use of these naturally designed reporters. Thus, an engineered interface to in vivo ABA signaling utilizing endogenous components as biosensors represents the best ready-to-use mechanism to detect micromolar (μM) level ABA in drought-stressed plants and could enable real time human-mediated mitigation of drought. These sensors would allow plants to report to farmers or automated irrigation systems to obtain point-of-mitigation. The PYL reporter proteins therefore present viable candidates to engineer a biosensor.

PYL-based ABA sensors have been investigated by designing recombinant proteins that incorporate fluorescent domains to enable optical sensing using principles such as Förster resonance energy transfer (FRET). One report demonstrated the quantification of μM concentrations of ABA in plants by obtaining the ratio of fluorescence intensities in two spectral regions from two fluorophores, one attached to a PYL and the other to a phosphatase.[4] Upon ABA binding, the phosphatase binds to the PYL to enable FRET, causing a decrease in fluorescence in one spectral region and increase in another. Other similar methods have been developed.[5] These pioneering works suggest that it is possible to develop sensitive optical sensors to detect ABA in plants.

Received: August 16, 2019
Accepted: November 8, 2019
Published: November 8, 2019

DOI: 10.1021/acs.analchem.9b03751
Anal. Chem. 2019, 91, 15644−15651

Other methods are available for the detection of bioavailable ABA, spanning from mass spectrometry[6,7] to antibody-based immunoassays such as commercially available ELISA[8,9] to electrochemical[10] and optical sensors not based on FRET.[11,12] The features of detection methods are given in Table 2, which is placed in the Discussion section.

We developed a new sensing mechanism using components of the ABA signaling pathway for the purpose of simplifying ABA detection. The principle behind this work is based on FRET quenching between fluorophore and quencher chemically conjugated to PYLs in heterodimers or homodimers. In this process, the quencher resonantly absorbs and dissipates the energy released from the excited fluorophore and reduces or eliminates fluorescence from the fluorophore. For efficient quenching through FRET, the fluorophore and quencher need to be located within a few nanometers of each other.[13] Our design takes advantage of the dimerization of the PYL receptors to establish this close proximity. The *Arabidopsis thaliana* genome encodes 14 PYL proteins, each with a different monomer−dimer dissociation equilibrium.[14] Without ABA, a significant portion of the PYL receptors stay in the dimeric form. In the presence of ABA, the equilibrium shifts toward PYL monomers which facilitates its binding to such proteins as phosphatase 2C Abscisic Acid Insensitive 1 (ABI1). For instance, the homodimeric receptor PYL3 has an equilibrium dissociation constant (K_d) of 7.76 μM, which increases to 52 μM when at saturating ABA concentrations.[15] This increase is attributed to a conformational change to the dimers from an initial *cis*-homodimer to a *trans*-homodimer upon ABA binding.[15,16] Therefore, the resulting dissociation of heterodimers leads to increased fluorescence in drought-stressed plants.

The new mechanism reported here employs fluorescence measurements in only a single spectral region, which allows the use of an optical band-pass filter and an inexpensive but sensitive detector rather than expensive and time-consuming data collection spectrometers. The design also offers the option of development of sentinel plants to report drought stress by conjugating small molecules to PYL proteins. In a different approach, such sensors can be used to detect small leaf samples for quick examinations in the field, overcoming the drawbacks of typical biological assays such as ELISA ABA kits that require extensive sample preparation and multiple experimental steps (Table 2).

The design employed in this work is described in Scheme 1 (top panel). PYL3 was used because it presents the highest dimeric dissociation constant.[14] A fluorescent molecule, Cy5.5, is chemically conjugated to a protein monomer to form PYL3−Cy5.5. In a separate synthesis, a quencher, BHQ3, is chemically conjugated to a monomer of the same protein species, forming PYL3−BHQ3 (mid panel). Equal amounts of PYL3−Cy5.5 and PYL3−BHQ3 monomers are mixed to ensure maximum optical signal changes upon ABA binding. With control of the synthesis conditions of these small molecule−protein fusions, one fluorophore or one quencher is conjugated to each PYL3 protein. Conjugation of fluorophores and quenchers are not anticipated to influence dimerization of PYL3, their binding of the ABA ligand, or the binding to other biomolecules such as the protein phosphatase 2C.

In this work, in vitro tests of the sensing mechanism described in Scheme 1 demonstrate that the sensor detects ABA through its interactions with the modified PYL3 proteins in water. The fluorescent signal intensifies with increasing ABA concentrations. These encouraging results suggest that this sensing mechanism can be employed to design biomolecule-based endogenous drought sensors to report drought stress when interfaced with external optical excitation and detection devices.

Scheme 1. Sensing Design To Detect ABA Molecules[a]

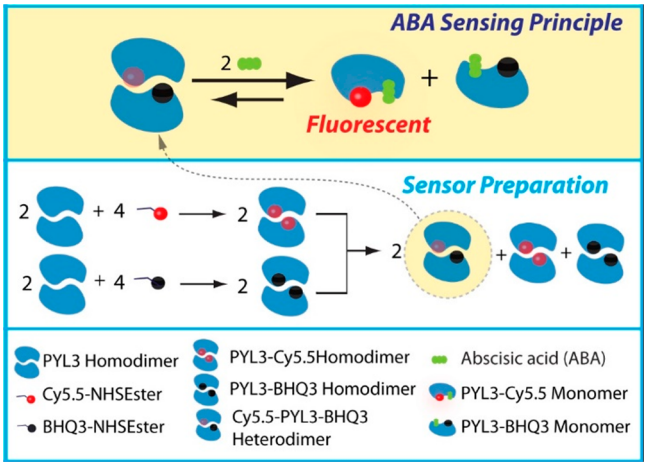

[a]The top panel displays the FRET-based quenching between a fluorophore Cy5.5 in PYL3−Cy5.5 and a quencher BHQ3 in PYL3−BHQ3. FRET quenching is shown as the dimmed Cy5.5 in the heterodimer. The middle panel describes the sensor preparation including Cy5.5−PYL3 and BHQ3−PYL3 monomers and homodimers. Self-quenching is represented by the slightly dimmed Cy5.5 in PYL3−Cy5.5 homodimers. Symbols are explained in the lower panel.

EXPERIMENTAL SECTION

Materials. pET28 and BL21[DE3] *E. coli* were used.[17] Growth media for *E. coli* (pET28) including LB Agar, tryptone, and yeast extract were purchased from BD. Sodium chloride, *N*-(2-hydroxyethyl)piperazine-*N*′-ethanesulfonic acid buffer, Tris buffer, triethanolamine, aluminum sulfate, sodium phosphate dibasic, sodium phosphate monobasic, Coomassie brilliant blue R, and polyacrylamide were purchased from Sigma-Aldrich. Kanamycin, chloramphenicol, isopropyl-β-D-thiogalactoside (IPTG), imidazole, and regenerated cellulose dialysis tubing were purchased from Thermo Fisher Scientific. A HisTrap HP column was purchased from GE Healthcare. A nonradioactive phosphatase assay system (Ser/Thr) was purchased from Promega. Cyanine5.5 NHS ester was purchased from Lumiprobe and BHQ3 NHS ester was purchased from Biosearch Technologies.

Protein Expression, Purification, and Dye Conjugation. pET28 *E. coli* with the required plasmids were used for expression and to prepare glycerol stocks with a final glycerol content of 25% for long-term storage at −80 °C. Protein expression was induced by cultivating *E. coli* in the presence of 0.1 mM IPTG. A preculture was grown overnight in a 12 mL culture tube at 37 °C. The main culture started with an optical density of 0.05−0.1 from the preculture. IPTG induction (0.1 mM final concentration) occurred after the *E. coli* reached an optical density of 0.3−0.5 at a wavelength of 605 nm and proceeded up to 6 h at 28 °C. After the expression was terminated on ice for approximately 5 min, the cells were centrifuged for 10 min at 4000*g*. The pellet was washed using 5 mL of purification buffer [20 mM phosphate buffered saline (PBS) and 500 mM NaCl at pH 7.4]. Protein extraction and

DOI: 10.1021/acs.analchem.9b03751
Anal. Chem. 2019, 91, 15644−15651

purification were carried out at 4 °C. The cells were suspended in 8 mL of denaturation purification buffer (20 mM PBS, 500 mM NaCl, 20 mM imidazole, and 8 M urea) and the proteins were extracted following an established protocol.[18] All media were autoclaved prior to use. The proteins were purified using a HisTrap HP 1 mL column, which was prepared by washing with 5 mL of 20% ethanol, 5 mL of Milli-Q water, and 5 mL of binding buffer (20 mM PBS and 500 mM NaCl at pH 7.4) at a flow rate of 1 mL/min. Proteins were applied at a flow rate of 0.15 mL/min. Five milliliters of binding buffer, 5 mL of wash buffer #1 (20 mM PBS, 500 mM NaCl, and 20 mM imidazole at pH 7.4), 5 mL of wash buffer #2 (20 mM PBS, 500 mM NaCl, and 40 mM imidazole at pH 7.4), and 5 mL of wash buffer #3 (20 mM PBS, 500 mM NaCl, and 60 mM imidazole at pH 7.4) were subsequently applied at 1 mL/min flow rate. Ten protein fractions were collected using 10 mL of elution buffer (20 mM PBS, 500 mM NaCl, and 500 mM imidazole at pH 7.4) at a flow rate of 1 mL/min. The column was restored by sequentially flushing with 5 mL of the elution buffer, Milli-Q water, and 20% ethanol at 1 mL/min. The elution fractions were tested using sodium dodecyl sulfate-polyacrylamide gel electrophoresis gels. Fractions with similar amounts of the protein were combined and the molar mass was verified using matrix-assisted laser desorption/ionization-mass spectrometry (MALDI). The protein concentration was determined using UV−vis absorption spectroscopy at 280 nm. The protein dimer has a molar extinction coefficient of 13 070 M^{-1} cm^{-1}. The absorption at 280 nm was background-corrected using the UV−vis absorption spectra (Figures 2A and 3A). Proteins were concentrated using reverse dialysis to obtain the final solutions. The purified homodimers were conjugated to Cy5.5 or BHQ3 NHS ester (Figure S1 in the Supporting Information) at an approximately 1:6 protein-to-dye ratio and a pH of 8.3. Prior to conjugation, 400 μL of 0.6 M sodium bicarbonate solution was added to 2 mL of approximately 1.9 mg/mL protein solution and the mixture was vortexed for less than a minute. Conjugation to Cy5.5 NHS ester or BHQ3 NHS ester was accomplished by adding 133 μL of 3.9 mM dye in dimethyl sulfoxide to 1.2 mL of the prepared protein solution at 4 °C and the mixture was allowed to react for 12 h. The products were purified by triple dialysis in 20 mM PBS. Concentration of the dye-conjugated proteins was determined using UV−vis absorption spectroscopy. Reverse dialysis was used to obtain Cy5.5- or BHQ3-conjugated proteins. Fisherbrand regenerated cellulose tubing with nominal MWCO of 12 000−14 000 was used for dialysis. One milliliter of Cy5.5 conjugated homodimer protein and 1 mL of BHQ3 conjugated homodimer protein solutions were mixed and incubated at 4 °C for 24 h to establish an exchange equilibrium for dye-conjugated heterodimers.

Characterization Methods. For fluorescence or molar mass measurements of the proteins as a function of ABA concentration, a 0.6 mL conjugated protein solution containing approximately equal amounts of protein conjugates was mixed with a 0.6 mL specified concentration of ABA (aq.) solution by vortexing and incubation for 20 min. UV−vis absorption measurements (Shimadzu UV−vis−NIR spectrophotometer, UV1700) were performed on PYL3−Cy5.5, PYL3−BHQ3, and a 1:1 mixture of PYL3 containing PYL3−Cy5.5 and PYL3−BHQ3. Fluorescence measurements (Yvon-Horiba FluoroMax-4) were performed on PYL3−Cy5.5, PYL3−BHQ3, and 1:1 mixture of PYL3 containing PYL3−Cy5.5 and PYL3−BHQ3 and as a function of ABA concentration. Static light scattering (SLS) (Malvern Zetasizer Nano S90 fitted with a 633 nm He−Ne laser) was used to determine the average molar mass. The mass of PYL3, PYL3−Cy5.5, and PYL3−BHQ3 were measured using Bruker UltraFlextreme MALDI TOF. Samples for MALDI-TOF measurements were prepared using a dried droplet method in a 2,5-dihydroxyacetophenone matrix.

RESULTS

After expression and purification of PYL3, the fluorophore conjugates were subsequently synthesized. PYL3 activity was tested and confirmed using the phosphatase assay, and the results indicate that recombinant protein−dye conjugates retained activity (Figure S2). MALDI measurements of pure PYL3 and postconjugation revealed three PYL3 protein complexes (Figure 1): purified PYL3 (blue line), conjugated

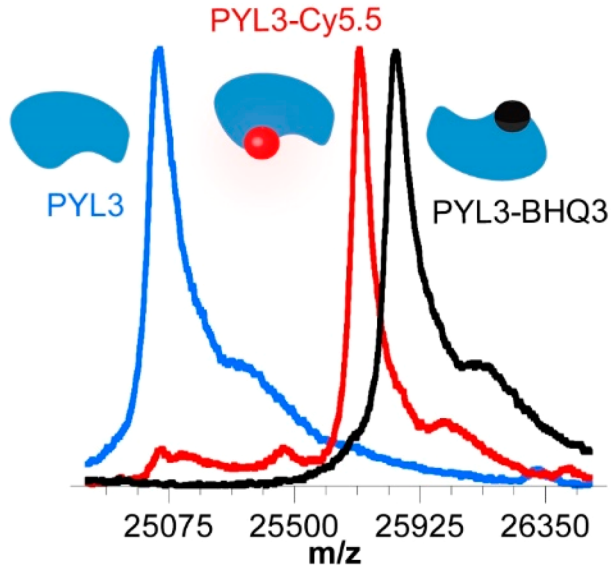

Figure 1. Conjugation of quencher BHQ3 and fluorophore Cy5.5 to PYL3. Mass-to-charge ratios of PYL3 (blue) and the conjugates of Cy5.5 (red) and BHQ3 (black) are shown. MALDI results suggest 100% reaction efficiency for conjugation reactions between PYL3 and dye molecules.

PYL3−Cy5.5 (red line), and conjugated BHQ3−PYL3 (black line). On average, only one Cy5.5 and one BHQ3 was conjugated to PYL3, respectively, at the concentration ratios of Cy5.5 and BHQ3 to PYL3 used in this work. Only conjugated PYL3 proteins were detected in postconjugation samples, suggesting 100% conjugation efficiency. MALDI, however, may favor the detection of Cy5.5−PYL3 or BHQ3−PYL3 over PYL3 because of high absorption of the desorption laser light by the dye molecules in the conjugated proteins.

When PYL3−Cy5.5 or PYL3−BHQ3 are dissolved in water, respectively, they form PYL3−Cy5.5 or PYL3−BHQ3 homodimers. For convenience, we call PYL3−Cy5.5 dimers or PYL3−BHQ3 dimers "homodimers". UV−vis absorption measurements covering wavelengths from 270 to 700 nm reveal absorption spectra of PYLs (peaked at 280 nm) and Cy5.5 and BHQ3 (peaked at 650 nm) (Figure 2A).

There was no fluorescence for PYL3 and BHQ3−PYL3 homodimers in aqueous solution, whereas fluorescence from PYL3−Cy5.5 homodimers (Figure 2B) was as similarly intense as that of Cy5.5 based on the data obtained from the UV−vis

DOI: 10.1021/acs.analchem.9b03751
Anal. Chem. 2019, 91, 15644−15651

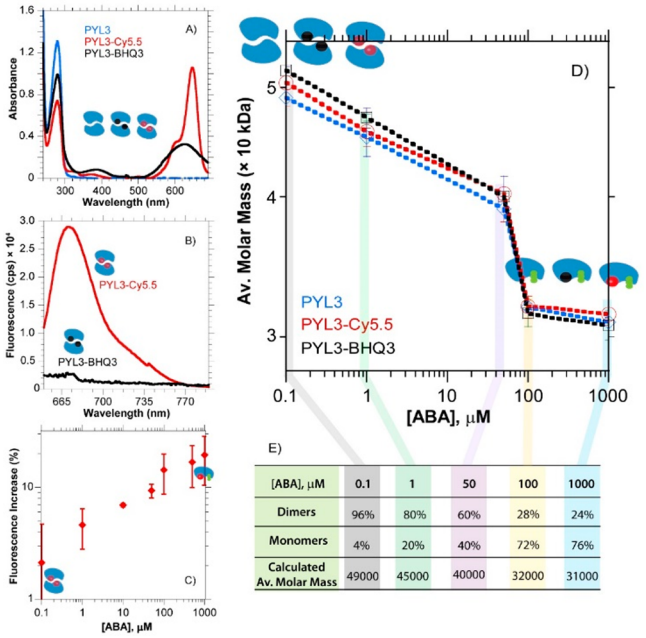

Figure 2. Characterization of fluorescence and quenching in PYL3, PYL3−Cy5.5, and PYL3−BHQ3 homodimers. (A) UV−vis absorption measurements of PYL3 (blue line), PYL3−Cy5.5 (red line), and PYL3−BHQ3 (black line). The data can be used to estimate conjugation reaction yield. (B) Fluorescence measurement of PYL3−Cy5.5 and PYL3−BHQ3. The latter yields little fluorescence. (C) Fluorescence of PYL3−Cy5.5 as a function of ABA concentrations, demonstrating self-quenching. (D) Average molar mass of the three species measured with SLS, which shows that ABA dissociates PYL3 dimers. Green = ABA ligand. (E) The calculated amounts of PYL3−Cy5.5 in dimer and monomer forms (in percentage) at 0.1, 1, 10, 100, and 1000 μM ABA using the data presented in (D). Even at 1 mM ABA, 24% of PYL3−Cy5.5 exists in the dimer form.

measurements. Figure 2C shows the results of a test of PYL3−Cy5.5 responses to the addition of ABA. On average, fluorescence intensity increased by 20% as the amount of ABA added to the mixture changed from 0.1 μM to 1 mM, suggesting at least a 20% self-quenching in PYL3−Cy5.5 homodimers in the absence of ABA in aqueous solution, a process similar to the reduced fluorescence in solutions of either high concentrations of fluorophores or high densities of fluorophores on the surface of nanoparticles.[19,20] This quenching efficiency will be used to estimate the quenching efficiency between Cy5.5 and BHQ3 in PYL3 heterodimers.

Results from static light scattering (SLS) measurements (Figure 2D) were used to estimate average molecular mass and hence percentage of dimers in solution (Figure 2E) based on molecular motion in solution, although the method is less accurate for determining molecular mass on the order of a few thousand atomic mass units.[21] As expected, all three proteins respond to ABA similarly, again suggesting that dye-conjugated PYL3 proteins respond similarly to PYL3 when binding to ABA. The average molecular mass of the species in solution decreased by nearly 20% as the ABA concentration increased from 100 nM to 40 μM, and by another 20% as ABA concentration increased from 50 to 100 μM. Seventy-eight micromolar proteins were used in each of these measurements. This means that more PYL3−Cy5.5 homodimers dissociate as more ABA is added to the solution of PYL3−Cy5.5. The SLS results show an average molecular mass of 50 kDa at 0.1 μM ABA and 30 kDa at 1 mM ABA. If a molecular mass of 51.6 kDa is chosen for homodimers and 25.8 kDa for monomers, then at 0.1 μM ABA only 6% of the PYL−Cy5.5 in solution is in the monomeric form, meaning 94% of PYL3−Cy5.5 is in the homodimer form. At 1 mM ABA, 76% of the PYL3−Cy5.5 is in the monomeric form and 24% of the PYL3−Cy5.5 stays in the homodimer form. These results are shown in Figure 2E.

By mixing of PYL3−Cy5.5 with PYL3−BHQ3 at an approximately 1:1 ratio in water, monomers, homodimers, and heterodimers coexist, as displayed in Scheme 1. We call PYL3−Cy5.5/PYL3−BHQ3 dimers "heterodimers" to distinguish them from homodimers of PYL3/PYL3, PYL3−Cy5.5/PYL3−Cy5.5, or PYL3−BHQ3/PYL3−BHQ3. UV−vis spectroscopy could be used to determine the equivalent concentrations of the proteins in solution (Figure 3A). The

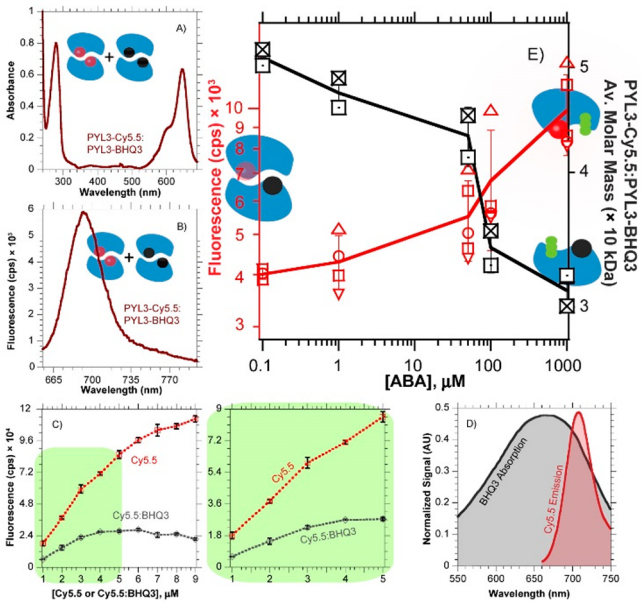

Figure 3. PYL3−Cy5.5 and PYL3−BHQ3 mixtures and their response as a function of ABA concentration. (A) UV−vis absorption profile. (B) Fluorescence profile. (C) Fluorescence of free BHQ3/Cy5.5 as a function of their concentrations. Attenuation of fluorescence is observed when Cy5.5 is mixed with BHQ3 (linear up to 4 μM for both components). (D) Absorption spectra of Cy5.5 and BHQ3. (E) Fluorescence response of the mixture as a function of ABA concentration (red symbols) and SLS measurements as a function of ABA concentration (black symbols). Fluorescence measurements employed five batches of PYL3, as represented by five sets of symbols. The fluorescence and molecular weight results both have the greatest signal changes between 40 and 100 μM ABA.

fluorescence, recorded as background or noise without ABA, comes from PYL3−Cy5.5, which belongs to PYL3−Cy5.5 monomers, PYL3−Cy5.5 homodimers, and PYL3−Cy5.5/PYL3−BHQ3 heterodimers (Figure 3B). Without ABA or at low ABA concentrations, most PYL3−Cy5.5 and PYL3−BHQ3 exist as dimers, similar to PYL3 or PYL3−Cy5.5. The measured fluorescence, therefore, is lower than the fluorescence of monomers because of self-quenching, quenching by BHQ3 in heterodimers through FRET and PYL3−BHQ3 monomers through attenuation. Because of these fluorescence reduction possibilities, it is difficult to use fluorescence to directly measure the concentration of PYL−Cy5.5. A more reliable way is to use absorption spectroscopy to determine the

DOI: 10.1021/acs.analchem.9b03751
Anal. Chem. 2019, 91, 15644−15651

conjugates concentration, which is also subjected to interference from concentration-dependent spectral changes. With use of the absorbance values at 280 and 643 nm for PYL3−Cy5.5 and PYL3−BHQ3 shown in Figure 3A and the absorbance values for Cy5.5 and BHQ3 aqueous solutions (shown in Figure S3), and if the conjugated Cy5.5 and BHQ3 absorb identically as in PYL3 proteins, the concentrations of Cy5.5 and BHQ3 in the samples shown in Figure 4A can be calculated as 4.65 and 4.00 μM, respectively.

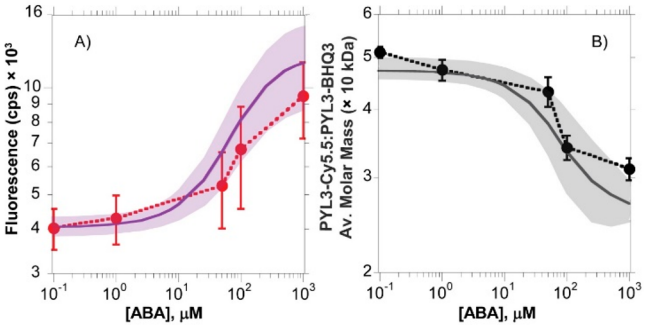

Figure 4. Simulations to predict the equilibrium concentrations of monomers and homodimers based on association/disassociation equations and binding constants. (A) Experimental (solid circles and dashed line) and theoretical (solid line and the shaded area) results of the total fluorescence signal as a function of ABA concentrations. The shaded area shows the range of fluorescence signal as the rate constants are varied. (B) Experimental SLS (dashed line) and simulated results of average molar mass. The shaded area shows the range of the average molar mass as the rate constants are varied.

Attenuation of fluorescence of Cy5.5 by free BHQ3 was investigated here as well. As the concentration of free BHQ3 and Cy5.5 increases in the mixture, attenuation of Cy5.5 fluorescence by BHQ3 is observed (Figure 3C, inset in Figure 3C, and Figure 3D). As a result, in the presence of BHQ3, Cy5.5 fluorescence is attenuated, even without FRET-based quenching or self-quenching. On the basis of the data shown in Figure 3C, there is nearly 64% attenuation to the fluorescence of 4 μM Cy5.5 by 4 μM BHQ3, decreasing the fluorescence intensity from 72 000 counts per second (cps) from pure Cy5.5 to 26 000 cps for the mixture of the same amount of Cy5.5 and BHQ3. This attenuation will be applied to explaining the results obtained using PYL-bound Cy5.5 and BHQ3.

SLS was used to quantify the percentages of heterodimers as a function of ABA concentration (black line and black symbols in Figure 3E). A 50 kDa average molecule mass was observed at 100 nM ABA, which corresponds to 98% of the PYL3 or conjugates being in the dimeric form, among which 25% are PYL3−BHQ3 homodimers, 25% are PYL3−Cy5.5 homodimers, and 50% are PYL3−BHQ3 and PYL3−Cy5.5 heterodimers (Scheme 1). As observed with addition of ABA to PYL3−Cy5.5 solutions, the amount of monomers increased upon addition of ABA. At 1 mM ABA, 80% of the PYL3 or conjugates were in the monomeric form. Table 1 shows the calculated percentages of monomers and dimers, including both hetero- and homodimers and the corresponding average molar masses at different ABA concentrations.

The fluorescence signal (red line and red symbols) of the mixture increases as ABA is added (Figure 3E), following an opposite trend to SLS measurements, which is expected. This increase should arise from more PYL3−Cy5.5/PYL3−BHQ3 monomers, which lead to decreased FRET quenching of Cy5.5 by BHQ3 in the heterodimers, and decreased self-quenching from Cy5.5 in PYL3−Cy5.5/PYL3−Cy5.5 homodimers as shown in Figure 2C. Assuming BHQ3 in PYL3−BHQ3 behaves similarly to free BHQ3 in solution, BHQ3 concentration-dependent attenuation (Figure 3D) is 64%; that is, fluorescence is decreased to 36% of the signal of pure Cy5.5, at the BHQ3-PYL3 concentration of 4.0 μM used in the measurements. FRET quenching of Cy5.5 by BHQ3 in heterodimers is assumed to be 90%, which is a slightly more conservative estimation than the 95% quenching efficiency obtained from Figures 2B and 3B. Here, 100% conjugation efficiency is used for the interpretation of the data. Table 1 shows the measured and estimated fluorescence intensities at different ABA concentrations using the quenching efficiencies obtained in this report. In calculating the final fluorescence intensities (total fluorescence in Table 1), we employ the self-quenching, FRET quenching, and BHQ3 concentration-dependent attenuation efficiency of 20%, 90%, and 73.2%, respectively. The corresponding factors are 0.8, 0.1, and 0.27, respectively. The BHQ3 concentration-dependent attenuation efficiency is slightly higher than 64%, measured using a mixture of 4 μM free Cy5.5 and 4 μM free BHQ3. The calculated final fluorescence intensities are within the standard deviations of the measured average values.

To further evaluate the measured results, we carried out theoretical simulations to predict equilibrium concentrations of monomers and dimers based on the rate equations and binding constants. Figure 4 displays results of simulations of binding

Table 1. Calculated Percentages of Dimers and Monomers at Different ABA Concentrations[a]

ABA concentration (μM)	0.1	1.0	40	100	1000
average molar mass (measured, amu)	51110	47410	43330	34050	31080
PYLs in dimers (hetero- and homodimers,%)	98	84	68	32	20
PYLs in monomers (%)	2	16	32	68	80
fluorescence (measured)	4015 ± 115	4292 ± 677	5301 ± 1204	6711 ± 2148	9494 ± 2164
fluorescence from Cy5.5 in monomers	630	5040	10080	21420	25200
fluorescence from Cy5.5 in homodimers	12348	10584	8568	4032	2520
fluorescence from Cy5.5 in heterodimers	1575	1350	1092	514	315
sum of Cy5.5 fluorescence	14553	16974	19741	25866	28035
total fluorescence	4045	4718	5488	7218	7793

[a]Self-quenching efficiency of 20% and BHQ3 concentration-dependent quenching shown in Figure 3C are used for calculations together with a calibrated fluorescence intensity of 79 653 cps from 4.65 μM Cy5.5. Units of fluorescence intensity are counts per second (cps). The values are calculated unless specified otherwise.

DOI: 10.1021/acs.analchem.9b03751
Anal. Chem. 2019, 91, 15644−15651

Table 2. Summary of the Features of Currently Available ABA Sensors

Key elements	Source of Samples	Detection Mechanism	Spectral regions (Range (nm))	Sensitivity (ppm/nM)	Steps/ Time[a]	Ref.
PYL3-Dye Conjugate	Transgenic or extract	Fluorescence	Single (680)	0.26/1000	2/20 min.	This work
FRET[b] (ABACUS)	Transgenic	Fluorescence	Two (485/535)	0.05–200/ 189–7.5×10^5	3/> 2 weeks	5
FRET (ABAleons)	Transgenic	Fluorescence	Two (440/527)	0.025–0.15/ 94–567	3/> 2 weeks	4
CALNNGK$_{(ABA)}$G - AuNP	Extract	UV-Vis	Whole (450–650)	0.00125-2.5/ 5–9.5×10^3	4/14 hours	22
Plasmonic	Extract	UV-Vis	Two (520/620)	0.09/340	4/25 hours	12
SPR[c] spectrometry (BIACore2000)	Purified Extract	SPR	Whole (N/A)	3×10^{-4} /1.1	2/74 min.	11
Immuno-PCR (q-IPCR)	Transgenic	PCR	N/A	0.99 ×10^{-6} / 4×10^{-3}	3/ 3.5 hours	23
Immuno Magnetic	Both	Chemilumines.	Whole (500–650)	2.6×10^{-6} –2.6/ 9.8×10^{-3}	3/3 hours	24
Immunoamplification (ELISA)	Transgenic	Optical	Whole (assay dependent)	0.16-10/ 605 – 3.8×10^4	8/15 hours	8, 25, 26
Impedance Immunosensor	Extract	Electrochemical	N/A	10^{-4}/3.8	3/3 hours	10, 27
Yeast-two-hybrid	Transgenic	cDNA screening	N/A	0.03/113	4/> 2 weeks	28
Microfluidics system	Extract	Interference fringe shift	Whole (Visible Range)	0.25/946	4/15 hours	29
Hormone reporter	Transgenic	Gene screening	N/A	0.4/1.5×10^3	3/24 hours	30
Hormone reporter	Transgenic	Gene activation	N/A	0.08 –26.4/ 302–10^4	2/24 hours	31
ABA receptor protein and phosphatase	In vivo	Fluorescence change	Single (527[d] or 509[e])	0.02/76	3/> 4 days	2
Radio Immunoassay (RIA)	Extract	Bound radioactivity	N/A	100 – 4000 pg	4/13 hours	32-34

and dissociation dynamics. The yield of conjugation is again assumed to be 100%, and the concentrations of PYL3−Cy5.5 and PYL−BHQ3 are 40 μM. Although conjugated PYL3 is used in the modeling, because conjugation has minimal influence on dimer formation or ABA binding, the results should be identical to those of PYL3. The kinetic rate equations containing the species of interest are shown in the Supporting Information. The rate constants are either obtained in the literature or assumed in this work. The assumed constants are varied to examine the response. Figure 4A (solid line (average values) and the shaded area (range or standard deviations)) shows the total fluorescence intensity of different combinations of fluorescence signals, with the signal being the sum of the rate constants of PYL3−Cy5.5, PYL3−Cy5.5−ABA, PYL3−Cy5.5/PYL3−Cy5.5, and PYL3−Cy5.5/PYL3−BHQ3. The dependency of fluorescence on ABA is similar in all cases, that is, fluorescence stays relatively constant at low ABA concentrations, below 1−10 μM. A semilinear relationship is established once the ABA concentration is between 10 and 1000 μM. This general trend agrees with the experimentally acquired dimer−ABA concentration profile pictured in Figure 3E (red line). The shaded area shows the range of the average fluorescence signal as the rate constants are varied (vide infra). Figure 4B (solid line) shows the average molecular masses of mixtures for different combinations of rate constants and ABA concentrations. The trend obtained from theoretical simulations closely resembles that of the experimental values (dashed line and solid round circles). The shaded area shows the range of average masses as the rate constants are varied. The k values used in the simulation are k_1 = 1.5−5.0, k_{-1} = 0.6−2.0, k_2 = 1.5−6.0, k_{-2} = 0.6−2.0, k_3 = 0.6−2.0, k_{-3} = 1.3−6.0, k_4 = 5.0−15.0, and k_{-4} = 7.2 × 10^{-6} − 5.2 × 10^{-5}. It is noticeable that k_1−k_3 are quite different from k_{-4}. This can be explained as k_1−k_3 are for dissociation of dimers in the presence of ABA whereas k_4 is for dissociation without ABA. Therefore, k_{-4} is equivalent to k_1−k_3 multiplying the ABA concentration, which is on the order of μM. As a result, k_{-4} is nearly 5 orders of magnitude smaller than k_1−k_3. The simulated total fluorescence (f) is calculated as $f = I_0(R_{[ABA]}/R_{No\ ABA})$, where I_0 = 3750 cps, which is the initial fluorescence signal of the heterodimer mixture measured prior to ABA addition. $R_{[ABA]}$ is the calculated fluorescence signal factor of heterodimer mixture as a function of ABA and R_{NoABA} is the factor without ABA. The R factors and the concentrations of different species obey the following relationship: R = ([PF−ABA] + 0.2 × [PFPQ] + 0.8 × [PFPF] + [PF]) where [PF−ABA] and [PF] are the concentrations of PYL3−Cy5.5−ABA and PYL3−Cy5.5, and [PFPQ] and

DOI: 10.1021/acs.analchem.9b03751
Anal. Chem. 2019, 91, 15644−15651

[PFPF] are the concentrations of PYL3−Cy5.5/PYL3−BHQ3 homodimers and PYL3−Cy5.5/PYL3−Cy5.5 homodimers.

Figure S4 shows the results of the average molar mass detection using 1.9 μM PYL3−Cy5.5 and PYL3−BHQ3 as a function of ABA concentrations. The inflection point of the transition is around 4 μM ABA, which is much lower than the 75 μM using 40 μM PYL3−Cy5.5/PYL3−BHQ3 shown in Figure 3E. Simulated results using the same set of rate constants as in Figure 4 agree with the experimental results. Although only average molar mass results are shown, we expect the fluorescence data follow the same anticorrelation trend as that shown in Figure 3E.

DISCUSSION

Here, we present a new method that can detect ABA through optical quenching between Cy5.5- and BHQ3-conjugated PYL3 monomers. The current design can detect μM concentrations of ABA in aqueous solutions. The detection of drought stress in plants through ABA detection in the μM range could be realized when the measured fluorescence is compared to the fluorescence levels from both healthy and stressed plants. The latter should emit higher fluorescence signals. The advantages are 2-fold: (1) a single dissociation reaction is needed to enable the sensing and (2) detection of fluorescence in a single wavelength region is needed. The results presented here provide a proof-of-principle for this new sensing mechanism. The current method is significantly simpler than the commercially available, antibody-based ELISA ABA kits, which require extensive sample treatments and preparations. Table 2 summarized the features of the current method and other published ones used to sense ABA in plants. The aim of the parameters given in Table 2 is to define field applicable sensors, which require fast detection, inexpensive equipment, and field applicability.

Several improvements can be made. First, if the conjugation efficiency is lower than 100%, then it should be maximized. Second, FRET quenching efficiency may be maximized. Our conjugation method does not have control over the location of Cy5.5 or BHQ3 conjugation. There are many amine sites on the surface of PYL3 monomers. All these sites could potentially be the binding site(s) for Cy5.5 or BHQ3. The random positions of fluorophore/quenching conjugation may lead to less efficient FRET quenching. If this quenching is 100%, then a third problem that needs to be solved is maximizing self-quenching efficiency. If there is strong self-quenching between Cy5.5 in homodimers, then the fluorescence signal without ABA can be minimized, hence increasing the detection sensitivity. For construction of practical sensors, a fourth improvement is needed, namely, to use fluorophore−quencher combinations such as Cy7.5 that emit in the near-infrared region to avoid background interference from chlorophyll emission.

Although the trends shown in the simulated results displayed in Figure 4 are in general agreement with the experimentally observed data, the measured SLS data still in part differ from the theoretically simulated results. The difference could be caused by using the SLS method to determine the average molar mass, especially at high ABA concentrations. The method may have intrinsic errors in determination of the molecular weight of monomers that have molecular weights of less than 30 000 g mol^{-1}.[21] A full calibration may be required for all the percentages of monomers and dimers and for all the conjugated as well as nonconjugated dimers. In addition, new methods and instruments need to be developed to understand the dissociation dynamics. Future work is required to fully calibrate all these combinations, including the actual yield of conjugation, free of bias.

The simulations predict a more complete dissociation than the experimentally measured values. Both fluorescence and molar mass simulation results present a highly correlated trend, suggesting that this discrepancy in the degree of dissociation of dimers does not depend on quenching calculations. Instead, experimentally, there are dimers that do not dissociate at the highest ABA concentrations, suggesting that some PYL3 may not be able to bind ABA. Future work will be needed to optimize PYLs to improve their ABA responses.

Additionally, the signal-to-noise ratios (SNR) should be improved prior to deployment in plants. The SNR obtained here are relatively low, at approximately 5.0, because the data acquisition time per data point was on the order of 5 s. In one of the published reports on using two wavelength detection, a <2% standard deviation (STD) was obtained, which suggests that SNR on the order of 50 can be obtained, at which 100−600 nM ABA can be detected.[4] Given that our current design can detect μM ABA (Figure 3E and Figure S4), it is reasonable to anticipate that further optimization will enable detection of lower, more physiologically relevant concentrations of ABA.

Future work is also needed to test this new mechanism in plants. Selectivity will need to be determined in vivo as other carotenoid-based molecules may compete with ABA to bind PYL. Another related question to answer is whether the dissociation constant for PYL3 dimers can be improved with respect to ABA binding.

CONCLUSIONS

A biosensor using native PYL3 proteins conjugated with Cy5.5 fluorophores or BHQ3 quenchers has been developed and tested here. Mixtures of equal amounts of PYL3−Cy5.5 and PYL3−BHQ3 protein conjugates are used as the biosensor. Fluorescence signal of the mixture increases by more than 50% upon mixing with 100 μM ABA, a phytohormone molecule that is produced in plants undergoing drought stress. The experimentally observed responses generally agree with the theoretical model trends. Future work includes in vivo tests and field studies to fully validate this biosensor.

q1aaa

ASSOCIATED CONTENT

Supporting Information

The Supporting Information is available free of charge at https://pubs.acs.org/doi/10.1021/acs.analchem.9b03751.

Results of phosphatase activity assay and the reaction steps and rate constants of the simulations (PDF)

AUTHOR INFORMATION

Corresponding Author

*E-mail: tguo@ucdavis.edu (T.G.).

ORCID

Ting Guo: 0000-0002-6700-0967

Author Contributions

The manuscript was written through contributions of all authors. All authors have given approval to the final version of the manuscript.

DOI: 10.1021/acs.analchem.9b03751
Anal. Chem. 2019, 91, 15644−15651

Notes

The authors declare no competing financial interest.

■ ACKNOWLEDGMENTS

This work is supported by the Innovation Institute for Food and Health (IIFH) at University of California, Davis. Partial funding was provided by a Howard Hughes Medical Institute Faculty Scholar fellowship to S.M.B. The authors thank Mengqi Su for her assistance.

■ REFERENCES

(1) Cutler, S. R.; Rodriguez, P. L.; Finkelstein, R. R.; Abrams, S. R. *Annu. Rev. Plant Biol.* **2010**, *61*, 651−679.
(2) Ma, Y.; Szostkiewicz, I.; Korte, A.; Moes, D.; Yang, Y.; Christmann, A.; Grill, E. *Science* **2009**, *324* (5930), 1064−1068.
(3) Park, S. Y.; Fung, P.; Nishimura, N.; Jensen, D. R.; Fujii, H.; Zhao, Y.; Lumba, S.; Santiago, J.; Rodrigues, A.; Chow, T. F. F.; Alfred, S. E.; Bonetta, D.; Finkelstein, R.; Provart, N. J.; Desveaux, D.; Rodriguez, P. L.; McCourt, P.; Zhu, J. K.; Schroeder, J. I.; Volkman, B. F.; Cutler, S. R. *Science* **2009**, *324* (5930), 1068−1071.
(4) Waadt, R.; Hitomi, K.; Nishimura, N.; Hitomi, C.; Adams, S. R.; Getzoff, E. D.; Schroeder, J. I. *eLife* **2014**, *3*, e01739.
(5) Jones, A. M.; Danielson, J. A. H.; ManojKumar, S. N.; Lanquar, V.; Grossmann, G.; Frommer, W. B. *eLife* **2014**, *3*, e01741.
(6) Jorge, T. F.; Mata, A. T.; Antonio, C. *Philos. Trans. R. Soc., A* **2016**, *374* (2079), 20150370.
(7) Chen, M. L.; Huang, Y. Q.; Liu, J. Q.; Yuan, B. F.; Feng, Y. Q. *J. Chromatogr. B: Anal. Technol. Biomed. Life Sci.* **2011**, *879* (13−14), 938−944.
(8) Daie, J.; Wyse, R. *Anal. Biochem.* **1982**, *119* (2), 365−371.
(9) Chen, X. J.; Lu, Y.; Tan, G. Y.; Cao, Z.; Liu, W.; Wang, B. M.; Zhang, M. C.; Li, Z. H. *Food Agric. Immunol.* **2016**, *27* (5), 624−642.
(10) Li, Y. W.; Xia, K.; Wang, R. Z.; Jiang, J. H.; Xiao, L. T. *Anal. Bioanal. Chem.* **2008**, *391* (8), 2869−2874.
(11) Badescu, G. O.; Marsh, A.; Smith, T. R.; Thompson, A. J.; Napier, R. M. *PLoS One* **2016**, *11* (3), e0152148.
(12) Wang, S.; Li, W.; Chang, K. K.; Liu, J.; Guo, Q. Q.; Sun, H. F.; Jiang, M.; Zhang, H.; Chen, J.; Hu, J. D. *PLoS One* **2017**, *12* (9), No. e0185530.
(13) Meer, B. W. v. d. *FRET - FFrster Resonance Energy Transfer: From Theory to Applications*; Wiley-VCH/Verlag GmbH & Co. KGaA: Weinheim, Germany, 2014.
(14) Hao, Q.; Yin, P.; Li, W. Q.; Wang, L.; Yan, C. Y.; Lin, Z. H.; Wu, J. Z.; Wang, J. W.; Yan, S. F.; Yan, N. *Mol. Cell* **2011**, *42* (5), 662−672.
(15) Zhang, X. L.; Zhang, Q.; Xin, Q.; Yu, L.; Wang, Z.; Wu, W.; Jiang, L.; Wang, G. Q.; Tian, W. L.; Deng, Z. Q.; Wang, Y.; Liu, Z.; Long, J. F.; Gong, Z. Z.; Chen, Z. Z. *Structure* **2012**, *20* (5), 780−790.
(16) Zhang, X. L.; Jiang, L.; Xin, Q.; Liu, Y.; Tan, J. X.; Chen, Z. Z. *Front Plant Sci.* **2015**, *6*, 88.
(17) Cutler, S. R.; Park, S.-Y.; Defries, A. U.S. Patent 9315821B2. 2016.
(18) Feliu, J. X.; Cubarsi, R.; Villaverde, A. *Biotechnol. Bioeng.* **1998**, *58* (5), 536−540.
(19) Reineck, P.; Gomez, D.; Ng, S. H.; Karg, M.; Bell, T.; Mulvaney, P.; Bach, U. *ACS Nano* **2013**, *7* (8), 6636−6648.
(20) Chen, W. Y.; Young, L. J.; Lu, M.; Zaccone, A.; Strohl, F.; Yu, N.; Kaminski Schierle, G. S.; Kaminski, C. F. *Nano Lett.* **2017**, *17* (1), 143−149.
(21) Oberlerchner, J. T.; Rosenau, T.; Potthast, A. *Molecules* **2015**, *20* (6), 10313−10341.
(22) Zhou, G. H.; Liu, Y. Z.; Luo, M.; Xu, Q. F.; Ji, X. H.; He, Z. K. *ACS Appl. Mater. Interfaces* **2012**, *4* (9), 5010−5015.
(23) Su, Y.; Li, W.; Huang, Z. G.; Wang, R. Z.; Luo, W. G.; Liu, Q.; Tong, J. H.; Xiao, L. T. *Plant Methods* **2018**, *14* (1), 104.
(24) Zhou, G. H.; Wang, P.; Yuan, J.; Qiu, T.; He, Z. K. *Sci. China: Chem.* **2011**, *54* (8), 1298−1303.
(25) Belefant, H.; Fong, F. *Plant Physiol.* **1989**, *91* (4), 1467−1470.
(26) Banowetz, G. M.; Hess, J. R.; Carman, J. G. *Hybridoma* **1994**, *13* (6), 537−541.
(27) Huang, Z.; Kabir, M. H.; Xiao, Y.; Liu, Q.; Tung, J.; Xiao, L. Principles and Practice of ABA Analysis. In *Abscisic Acid: Metabolism, Transport and Signaling*; Zhang, D. P., Ed.; Springer Science+Business Media: Dordrecht, 2014; pp 431−446.
(28) Kanno, Y.; Hanada, A.; Chiba, Y.; Ichikawa, T.; Nakazawa, M.; Matsui, M.; Koshiba, T.; Kamiya, Y.; Seo, M. *Proc. Natl. Acad. Sci. U. S. A.* **2012**, *109* (24), 9653−9658.
(29) Song, C.; Che, C.; Che, X.; Wang, W.; Que, L. Detection of Plant Hormone Abscisic Acid (ABA) Using an Optical Aptamer-Based Sensor with a Microfluidics Capillary Interface. In *2017 IEEE 30th International Conference on Micro Electro Mechanical Systems (MEMS)*, Las Vegas, NV, USA, January 22−26, 2017; IEEE: Piscataway, NJ, 2017; pp 370−373.
(30) Schroeder, S. R.; White, C. W.; Jones, T. N.; Hendry-Hofer, T. B.; Day, B. J.; Eaton, S. S. *Appl. Magn. Reson.* **2011**, *40* (1), 125−134.
(31) Christmann, A.; Hoffmann, T.; Teplova, I.; Grill, E.; Muller, A. *Plant Physiol.* **2005**, *137* (1), 209−219.
(32) Quarrie, S. A.; Whitford, P. N.; Appleford, N. E. J.; Wang, T. L.; Cook, S. K.; Henson, I. E.; Loveys, B. R. *Planta* **1988**, *173* (3), 330−339.
(33) Liu, Y. G.; Ye, N. H.; Liu, R.; Chen, M. X.; Zhang, J. H. *J. Exp. Bot.* **2010**, *61* (11), 2979−2990.
(34) Su, Y. H.; Su, Y. X.; Liu, Y. G.; Zhang, X. S. *Plant Growth Regul.* **2013**, *69* (2), 167−176.

DOI: 10.1021/acs.analchem.9b03751
Anal. Chem. 2019, 91, 15644−15651